First-principles calculations of 5d atoms doped hexagonal-AlN sheets: Geometry, magnetic property and the influence of symmetry and symmetry-breaking on the electronic structure*

Zhang Zhao-Fu(张召富), Zhou Tie-Ge(周铁戈)†, Zhao Hai-Yang(赵海洋), and Wei Xiang-Lei(卫湘蕾)

College of Information Technical Science, Nankai University, Tianjin 300071, *China*

(Received 13 April 2013; revised manuscript received 17 June 2013; published 12 November 2013)

The geometry, electronic structure and magnetic property of the hexagonal AlN (h-AlN) sheet doped by 5d atoms (Lu, Hf, Ta, W, Re, Os, Ir, Pt, Au and Hg) are investigated by first-principles calculations based on the density functional theory. The influence of symmetry and symmetry-breaking is also studied. There are two types of local symmetries of the doped systems: C_{3v} and D_{3h}. The symmetry will deviate from exact C_{3v} and D_{3h} for some particular dopants after optimization. The total magnetic moments of the doped systems are $0\mu_B$ for Lu, Ta and Ir; $1\mu_B$ for Hf, W, Pt and Hg; $2\mu_B$ for Re and Au; and $3\mu_B$ for Os and Al-vacancy. The total densities of state are presented, where impurity energy levels exist. The impurity energy levels and total magnetic moments can be explained by the splitting of 5d orbitals or molecular orbitals under different symmetries.

Keywords: hexagonal-AlN sheet, first-principles calculations, 5d atoms, symmetry and symmetry-breaking

PACS: 68.65.–k, 71.15.Mb, 71.20.–b, 73.20.Hb **DOI:** 10.1088/1674-1056/23/1/016801

1. Introduction

In recent years, low-dimensional systems such as graphene,[1,2] carbon nanotube,[3] h-BN sheet[4] and BN nanotube[5] have been widely studied because of their special geometry structures and excellent electronic properties. Low-dimensional systems can be applied in various fields, such as condensed matter physics, spintronics[6] and nano electronics. The III–V compounds are important semiconductors and the corresponding low-dimensional phases are becoming a focus of research.[7–12] Hexagonal-AlN (h-AlN) has attracted much attention.[13–17] The properties of h-AlN, such as the geometry, electronic structure and magnetic properties, can be tuned by absorbing or doping.[18,19] Qiao *et al.*[20] investigated the electronic and structural properties of the N-vacancy in AlN nanowires. Zhang *et al.*[21] studied the structural, thermodynamic and electronic properties of zinc-blende AlN with first-principles calculations. de Almeida Junior *et al.*[22] explored the most typical defects in h-AlN, including vacancies, antisite defects and impurities including C and Si.

Besides low-dimensional systems, heavy 5d atoms are becoming more and more attractive for researchers. In 2009, Shitade *et al.*[23] reported the quantum spin Hall effect in Na_2IrO_3. In 2012, Zhang *et al.*[24] reported the electrically tunable quantum anomalous Hall effect in graphene decorated with 5d transition-metal adatoms. Hu *et al.*[25] reported the giant topological insulator gap in graphene with 5d adatoms. It can be seen that two-dimensional systems doped by 5d atoms are worth a detailed study for both theory and practical application.

A 5d atom's radius is similar to that of an Al atom, making it easier to realize a doped system; so we investigate the geometry, electronic structure and magnetic properties of a 5d atom doped h-AlN sheet, in which one 5d transition metal atom (Lu, Hf, Ta, W, Re, Os, Ir, Pt, Au or Hg) substitutes for one Al atom. First-principles calculations based on the density functional theory (DFT)[26,27] are adopted. In particular, the electronic structure and magnetic properties are explained by analyzing the splitting of 5d orbitals or molecular orbitals under different symmetries. In this paper, we report our calculation method, results and analysis in detail.

2. Calculation method

The framework adopted in the calculations is the DFT implemented in the SIESTA (Spanish Initiative for Electronic Simulations with Thousands of Atoms) code.[28–30] Perdew, Burke and Ernzerhof (PBE)'s generalized gradient approximation (GGA)[31] is adopted to describe the electron exchange correlation. The valence electron wave functions are expanded in a localized numerical atomic orbital basis set: a double-ζ basis plus polarization orbitals (DZP). The grid in real space employs a mesh cut-off of 240 Ry. The configurations of the valence electrons are as follows: Lu: $5d^16s^2$, Hf: $5d^26s^2$, Ta: $5d^36s^2$, W: $5d^46s^2$, Re: $5d^56s^2$, Os: $5d^66s^2$, Ir: $5d^76s^2$, Pt: $5d^96s^1$, Au: $5d^{10}6s^1$ and Hg:$5d^{10}6s^2$. The calculation is carried out in two steps. First, the geometry of the doped system is fully optimized. Second, the electronic structure and mag-

*Project supported by Tianjin Natural Science Fund, China (Grant No. 13JCQNJC00500), the Fundamental Research Funds for the Central Universities, China (Grant No. 65012031), and Tianjin Key Technology R&D Program, China (Grant No. 11ZCKFGX01300).

†Corresponding author. E-mail: zhoutg@nankai.edu.cn

© 2014 Chinese Physical Society and IOP Publishing Ltd

netic properties of the optimized system are calculated with higher accuracy. In the geometry optimization, the adopted 5×5×1 k mesh results in a convergence of 0.01 eV and the changes in the total energy between successive iteration steps are smaller than 10^{-4} eV. The relaxation criterion of the residual Hellmann–Feynman force is 0.02 eV/Å. In the static calculation, the adopted 7×7×1 k mesh results in a convergence of 0.001 eV and the changes in the total energy are smaller than 10^{-6} eV. Other parameters are set as those in the geometry optimization. To obtain clear and accurate density of states, the range of energy is from −15.00 eV to 5.00 eV and there are 5000 points in total.

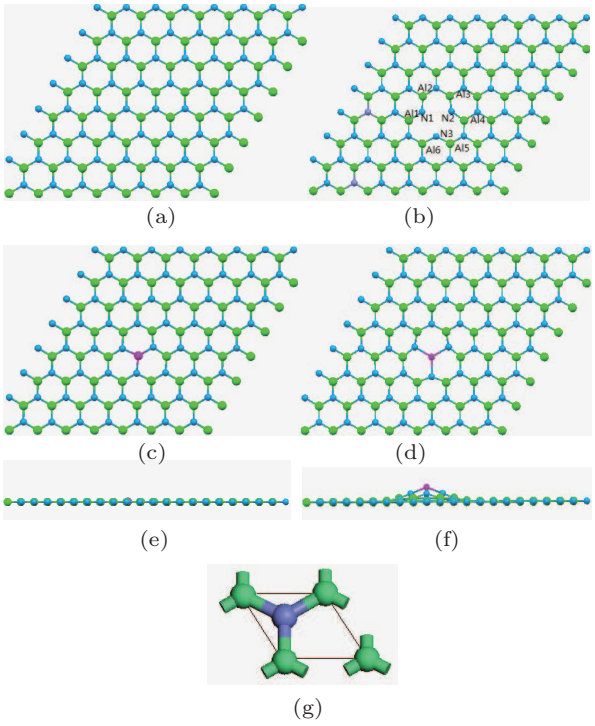


Fig. 1. (color online) Supercells of perfect AlN (a), V_{Al} (b), Os_{Al} ((c) top view, (e) side view) and Hg_{Al} ((d) top view, (f) side view) sheet and (g) the h-AlN unit cell (the green atom is the Al atom, the blue atom is the N atom and the pink atom is the impurity atom).

There is one N atom and one Al atom in the unit cell (see Fig. 1(g)) of the h-AlN sheet. To reduce the impact of periodicity, a 7×7 supercell is adopted, which includes 49 Al atoms and 49 N atoms. In our calculation, the distance between two neighboring h-AlN sheets is 18 Å. One 5d atom substitutes for one Al atom in the supercell; there are ten different kinds of doped systems (abbreviated as Lu_{Al}, Hf_{Al}, Ta_{Al}, W_{Al}, Re_{Al}, Os_{Al}, Ir_{Al}, Pt_{Al}, Au_{Al} and Hg_{Al}; $5d_{Al}$ represents all the doped systems). The perfect h-AlN sheet and an h-AlN sheet with Al-vacancy (V_{Al}) are also studied for comparison. The ten doped systems are mainly of D_{3h} (Ta_{Al}, W_{Al}, Re_{Al}, and Os_{Al}) or C_{3v} (Lu_{Al}, Hf_{Al}, Ir_{Al}, Pt_{Al}, Au_{Al}, and Hg_{Al}) symmetry. The structures of the systems mentioned above are shown in Fig. 1. Figure 1(a) displays the perfect h-AlN sheet. Figure 1(b) displays the h-AlN sheet with Al-vacancy (V_{Al}). Figures 1(c) and 1(d) display the top views of Os (D_{3h}) substituting for Al and Hg (C_{3v}) substituting for Al in the h-AlN sheet, respectively. Figures 1(e) and 1(f) display the corresponding side views, which illustrate the geometry and symmetry.

3. Results and discussion

3.1. Geometry

The optimized Al–N bond length is 1.826 Å and the distance between two neighboring N atoms is 3.161 Å, which are in good agreement with the calculated results given in Refs. [22], [32] and [33]. For V_{Al}, the surrounding three N atoms get away from each other. As shown in Fig. 1(b), the distances of N1–N2, N2–N3 and N3–N1 are 3.415 Å, 3.416 Å and 3.258 Å, respectively. Besides, the length of the Al–N bond surrounding the V_{Al} becomes smaller. The lengths of Al1–N1, Al2–N1, Al3–N2, Al4–N2, Al5–N3 and Al6–N3 are 1.820 Å, 1.826 Å, 1.798 Å, 1.798 Å, 1.825 Å and 1.821 Å, respectively. It is clear that there is a deviation from the exact D_{3h} symmetry. Table 1 lists the interatomic distance and binding energy of the h-AlN sheet doped with 5d atoms after optimization.

Table 1. Interatomic distance and binding energy of $5d_{Al}$ and V_{Al}.

Doping atom	h–5d/Å	D–N1/Å	D–N2/Å	D–N3/Å	E_b/eV
Lu	1.766	2.278	2.278	2.279	11.6768
Hf	0.716	2.044	2.044	2.044	13.8601
Ta	0.013	1.966	1.965	1.966	12.9481
W	0.004	1.929	1.998	1.928	11.5065
Re	0.203	1.955	1.954	1.955	10.4779
Os	0.026	1.955	1.923	1.956	9.8594
Ir	1.086	2.029	2.029	2.029	9.2782
Pt	1.287	2.110	2.091	2.109	6.4708
Au	1.559	2.247	2.246	2.247	4.9895
Hg	1.572	2.323	2.324	2.323	4.6078

In Table 1, the h–5d represents the distance between the substitutional 5d atom and the h-AlN sheet plane; D–N1, D–N2 and D–N3 represent the distances between the 5d atom and the nearest neighboring three N atoms, respectively. The h–5d indicates the deformation of the doped h-AlN sheets. It can be seen that the h-AlN sheets doped with Ta, W and Os tend to have a D_{3h} local symmetry, while the sheets doped with Lu, Hf, Ir, Pt, Au and Hg have a larger deformation and tend to have a C_{3v} local symmetry. For Re doping, the symmetry is closer to D_{3h}. Furthermore, the symmetry of the sheets doped with W and Os has a deviation from D_{3h}, while that of the sheet doped with Pt has a deviation from C_{3v}, because D–N1, D–N2 and D–N3 are not equivalent. This deviation will have a significant impact on the electronic structure and magnetic properties. A detailed discussion will be made in the following. The binding energy E_b is given by the following formula:

$$E_b = E_{VAl} + E_{5d} - E_{total}, \quad (1)$$

where E_{VAl} is the total energy of the AlN sheet with one Al vacancy, $E_{5\mathrm{d}}$ is the energy of one independent 5d atom and E_{total} is the total energy of the 5d atom doped h-AlN sheet after optimization. As illustrated in Table 1, the values of E_{b} are all positive, which indicates the stable adsorption of impurity atoms.

An obvious decrease of binding energy can be seen, which indicates the weakening of the bonds. The binding energy of Pt, Au and Hg is much smaller, it reflects much weaker bonds.

3.2. Electronic structure

Figure 2 displays the total densities of state (DOS) of the systems being studied. The dashed line in the figure represents the Fermi energy E_{F}, which is shown in Table 2.

Table 2. Fermi levels of all the supercell systems.

System	Lu_{Al}	Hf_{Al}	Ta_{Al}	W_{Al}	Re_{Al}	Os_{Al}	Ir_{Al}	Pt_{Al}	Au_{Al}	Hg_{Al}	AlN	V_{Al}
E_{F}/eV	–4.3681	–3.1508	–2.9960	–2.9959	–3.0579	–3.6765	–4.2564	–4.8477	–5.2486	–5.3886	–4.2874	–5.3671

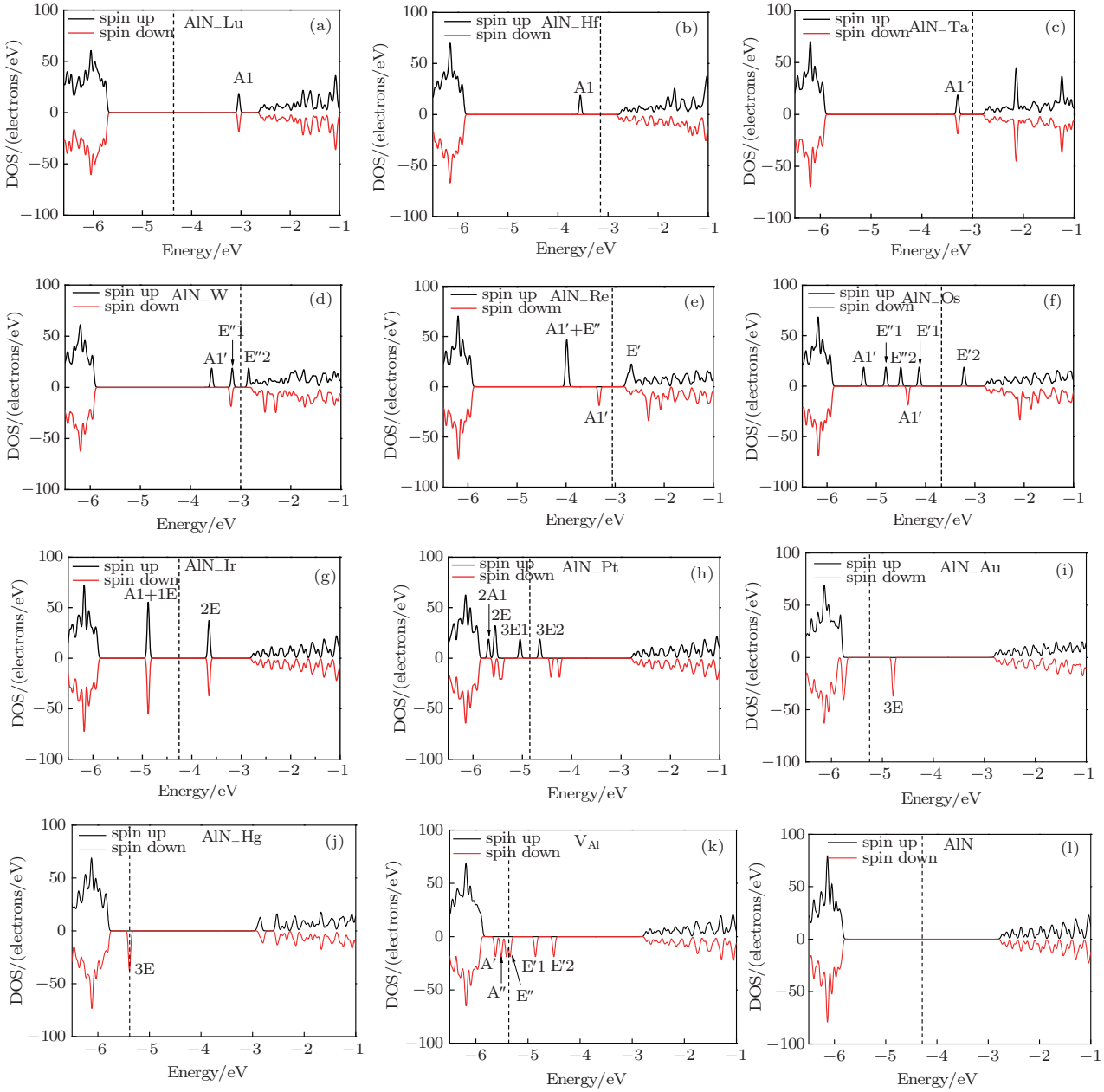


Fig. 2. (color online) Densities of states of (a) Lu_{Al}, (b) Hf_{Al}, (c) Ta_{Al}, (d) W_{Al}, (e) Re_{Al}, (f) Os_{Al}, (g) Ir_{Al}, (h) Pt_{Al}, (i) Au_{Al}, (j) Hg_{Al}, (k) V_{Al}, (l) perfect AlN (the dashed line represents Fermi level, the black curve represents total DOS of spin up and the red curve represents total DOS of spin down).

As shown in Fig. 2, there are obvious impurity energy levels in the band gap. To show the generation of the impurity levels, we consider the splitting of the 5d orbitals or molecular orbitals under different symmetries.

For Lu, Hf and Ir, when doped in AlN, the symmetry is strict C_{3v}, which contains three irreducible representations, namely, A1 (one-dimensional), A2 (one-dimensional) and E (two-dimensional). The splitting of 5d orbitals under the symmetry is illustrated in Fig. 3. The d_z^2 orbital forms the basis of A1 irreducible representation and constitutes a single degenerate level. The ($d_{x^2-y^2}$, d_{xy}) and (d_{xz}, d_{yz}) are both of E symmetry; they will mix further and produce two double degenerate levels of 1E and 2E. The splitting of 1E and 2E is relatively large, since there is a further mix between ($d_{x^2-y^2}$, d_{xy}) and (d_{xz}, d_{yz}). We can rank the orbitals out from the lowest to the highest according to the energy as A1, 1E and 2E.

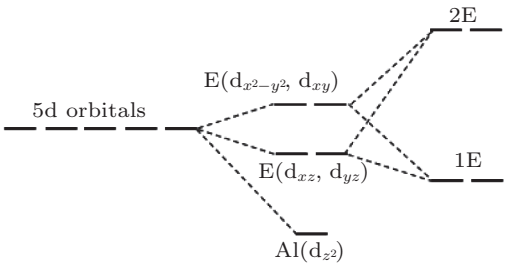


Fig. 3. The splitting of 5d orbitals under C_{3v} local symmetry.

The valence electron configuration of the Lu atom is $5d^16s^2$; its three valence electrons will be deprived by the three N atoms when doped in the h-AlN system. Then the number of d electrons is zero, which results in a total magnetic moment of zero. The A1 energy level is at −3.055 eV, as can be obviously observed in Fig. 2(a).

For the Hf atom, the valence electron configuration is $5d^26s^2$, there is one d electron left when doped in AlN. The only d electron fills the A1 orbital, making it half occupied and the total magnetic moment will be $1\mu_B$. It can be seen from Fig. 2(b) that the A1 energy level appears at −3.563 eV of the spin-up channel. Similarly, the Ir atom has a valence electron configuration of $5d^76s^2$ and has six d electrons left when doped in h-AlN. Because of the large gap between 1E and 2E, the six electrons will fully occupy the A1 and 1E orbitals (both spin-up and spin-down orbitals are fully occupied), which makes the total magnetic moment zero. The two impurity energy levels, A1 and 1E (occupied), are both at −4.876 eV, as can be seen in Fig. 2(g). The 2E level at −3.655 eV is vacant.

For Ta, W, Re and Os doped systems, the local symmetry is nearly D_{3h}, which contains six irreducible representations, namely A1′, A1″, A2′, A2″, E′ and E″. The splitting of 5d orbitals is shown in Fig. 4. The d_z^2 is of A1′ symmetry and constitutes a single degenerate energy level of A1′. The ($d_{x^2-y^2}$, d_{xy}) is of E′ symmetry and the (d_{xz}, d_{yz}) is of E″ symmetry. Due to the different symmetries, E′ and E″ have no hybridization. The splitting of E′ and E″ is small compared with that in the situation with the C_{3v} symmetry where a further hybridization exists. On the contrary, the splitting of A1 and E″ is large. Furthermore, the deviation of W_{Al} and Os_{Al} from the precise D_{3h} symmetry results in a removal of the degeneracy of E′ and E″ and four singlet states E″1, E″2, E′1 and E′2 emerge.

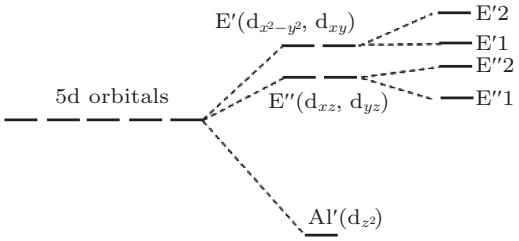


Fig. 4. The splitting of 5d orbitals under D_{3h} local symmetry.

The valence electron configuration of the Ta atom is $5d^36s^2$; it has two d electrons left when doped in h-AlN. The two d electrons with opposite spins both fill the A1′ state as a result of the large energy gap between A1′ and E″. So the total magnetic moment will be 0. The A1 energy level can be observed at −3.354 eV in Fig. 2(c). For W, there are three d electrons left when doped in h-AlN. According to the analysis above, two electrons with opposite spins will fill the A1′ state and the third one is situated on the E″ level. Since E″ is a double degenerate level, it is neither fully occupied nor half filled, which results in a geometry distortion from the exact D_{3h} symmetry according to the Jahn–Teller effect. So the E″ level is split into two singlet states E″1 and E″2. The system's total magnetic moment will be $1\mu_B$. The A1′, E″1 and E″2 energy levels can be seen at −3.560 eV, −3.170 eV and −2.809 eV in Fig. 2(d), respectively. For Re_{Al}, the deviation from the exact symmetry is much smaller and the degeneracy of E′ and E″ is preserved. There are four d electrons left when Re is doped in h-AlN. Two electrons with opposite spins will fill the A1′ state and the other two electrons with parallel spin will half fill the E″ state. So the total magnetic moment will be $2\mu_B$. In Fig. 2(e), the A1′ (spin-up) and E″ (spin-up) levels overlap with each other at −4.010 eV. The A1′ (spin-down) and E′ (spin-up) levels are located at −3.351 eV and −2.679 eV, respectively. For Os, there are five d electrons left when replacing Al. Two d electrons with opposite spins fill the A1′ level. Two electrons with parallel spin half fill the E″ level. The last electron is situated on the E′ level. The E′ is a double-degenerate level and the occupancy of one electron results in a geometry distortion and the splitting of the E′ level. As a consequence, the A1′, E″1, E″2, A1′, E′1 and E′2 levels can be observed at −5.261 eV, −4.810 eV, −4.501 eV, −4.351 eV, −4.121 eV and −3.220 eV in Fig. 2(f), respectively.

For Pt, Au and Hg, the valence is not +3 and there is a strong hybridization between the 5d orbitals and the closest N atom orbitals. So, instead of the splitting of 5d orbitals, a molecular orbital theory is more suitable for these systems. The doped systems are all of C_{3V} symmetry and the molecular orbital energy level diagram is shown in Fig. 5. If one Al atom is moved away from the sheet, the surrounding three N atoms form three σ dangling bonds, which can be decomposed into its irreducible components A1 and E under the C_{3V} symmetry. The 5d orbitals of the impurity atoms can be decomposed into one A1 and two E irreducible components. The 6s orbital naturally has the symmetry of A1. Only orbitals with the same symmetry can hybrid with each other, thus generating three molecular levels with A1 symmetry and three molecular levels with E symmetry, laying out as 1A1, 1E, 2A1, 2E, 3E and 3A1 in order. If the system deviates from the exact C_{3V} symmetry, for example Pt_{Al}, the double degenerate levels will split into single degenerate levels. As shown in Fig. 5, the level 1E splits into 1E1 and 1E2, the level 2E splits into 2E1 and 2E2 and the level 3E splits into 3E1 and 3E2.

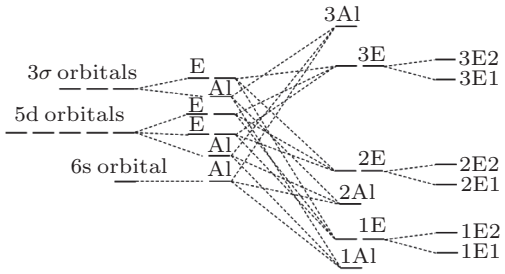


Fig. 5. Schematic molecular orbital energy level diagram for Pt_{Al}, Au_{Al} and Hg_{Al}.

For Pt_{Al}, there are 13 valence electrons in total, taking the three unpaired electrons of the surrounding N atoms into account. The electrons will fill in the molecular orbitals from lower energy to higher energy. Due to the large gap between the 2E and 3E levels, the 3E orbital cannot be filled in until the 1A1, 1E, 2A1 and 2E levels are fully occupied by 12 electrons. So there is one electron in the 3E level and the total magnetic moment should be $1\mu_B$. The 3E state is neither fully occupied nor half filled, which will cause a deviation from the exact C_{3V} symmetry and the split of degenerate states. The 2A1, 2E, 3E1 and 3E2 can be seen at -5.682 eV, -5.541 eV, -5.041 eV and -4.640 eV in Fig. 2(h), respectively. There is one more electron in the Au_{Al} system, filling in the 3E states, so the 3E orbital is half-occupied and the geometry is of nearly exact C_{3V} symmetry. The total magnetic moment will be $2\mu_B$. It can be seen from Fig. 2(i) that the 3E (spin-down) level stays empty at -4.766 eV. The Hg_{Al} has one more electron than Pt_{Al} and the additional electron fills in the 3E level (spin-down), so the total magnetic moment will be $1\mu_B$.

For the h-AlN sheet with an Al vacancy, both the three σ dangling bonds and the p_z orbits of the surrounding N atoms should be considered, because the lack of three electrons (equivalent to three holes) may have a great influence on the electronic structure. The local symmetry has a derivation from the exact D_{3h}. From the schematic molecular orbital energy level diagram shown in Fig. 6, we can see that the three σ orbitals are decomposed into A′1 and E′ irreducible components, while the three p_z orbitals are decomposed into A1″ and E″. The overlap among the three p_z orbitals is small, so the splitting of A1′ and E′ is small. On the contrary, the overlap among the three σ orbitals is large, so the hybridization is more obvious, resulting in a large split. Taking the system's deviation from the D_{3h} symmetry into consideration, the E′ level splits into two single degenerate levels E′1 and E′2, while the split of E″ is not obvious.

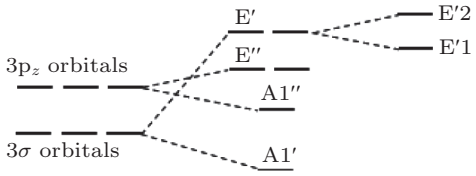


Fig. 6. Schematic molecular orbital energy level diagram for V_{Al}.

The three holes fill in the E″, E′1 and E′2 and the magnetic moment should be $3\mu_B$. The A1′, A1″, E″, E′1 and E′2 (spin down) levels are illustrated at -5.652 eV, -5.501 eV, -5.361 eV, -4.891 eV and -4.440 eV in Fig. 2(k), respectively.

3.3. Magnetic properties

3.3.1. Total and local magnetic moments

Table 3 shows the total magnetic moments (M_{total}) and local magnetic moments of the 5d atoms (M_{5d}) and the surrounding N atoms (M_{N1}, M_{N2}, M_{N3}). The results of V_{Al} are also given in the table for comparison.

Table 3. Total and local magnetic moments.

System	M_{total}/μ_B	M_{5d}/μ_B	M_{N1}/μ_B	M_{N2}/μ_B	M_{N3}/μ_B
Lu_{Al}	0	0	0	0	0
Hf_{Al}	1	1.060	–0.038	–0.038	–0.038
Ta_{Al}	0	0	0	0	0
W_{Al}	1	0.864	–0.006	0.078	–0.006
Re_{Al}	2	1.663	0.065	0.066	0.065
Os_{Al}	3	2.381	0.094	0.117	0.094
Ir_{Al}	0	0	0	0	0
Pt_{Al}	1	0.427	0.244	–0.001	0.242
Au_{Al}	2	0.307	0.506	0.503	0.505
Hg_{Al}	1	–0.009	0.280	0.277	0.281
V_{Al}	3	–	0.904	0.896	0.906

Table 3 illustrates that different doped systems have different total magnetic moments, which is consistent with the preceding analysis: 0 for Lu_{Al}, Ta_{Al} and Ir_{Al}; $1\mu_B$ for Hf_{Al}, W_{Al}, Pt_{Al} and Hg_{Al}; $2\mu_B$ for Re_{Al} and Au_{Al}; $3\mu_B$ for Os_{Al} and V_{Al}. Gao *et al.*[34] and Ran *et al.*[35] have investigated Fe and

Cu doped AlN, respectively. Their experimental results proved the existence of magnetism in the doped systems. Since an Os atom has the same valance electron configuration with an Fe atom, the existence of magnetism in Os doped AlN can be justified indirectly. Similarly, Au and Cu atoms share the same valance electron configuration, so the existence of magnetism in Au doped AlN can also be proved.

For Pt_{Al}, Au_{Al} and Hg_{Al}, the local magnetic moments of the surrounding three N atoms are relatively large, which reflects that the orbitals of the 5d and N atoms have a large hybridization and that it is reasonable to employ the molecular orbital theory. Hybridization in other doped systems is not so remarkable, so we can just consider the splitting of the 5d orbitals.

3.3.2. Spin density

Figure 7 shows the spin density maps of the systems with nonzero total magnetic moments. As seen in the spin density maps, large local magnetic moments are found in the surrounding N atoms of the Pt, Au and Hg doped systems, while those of the other systems are small, which is consistent with Table 3.

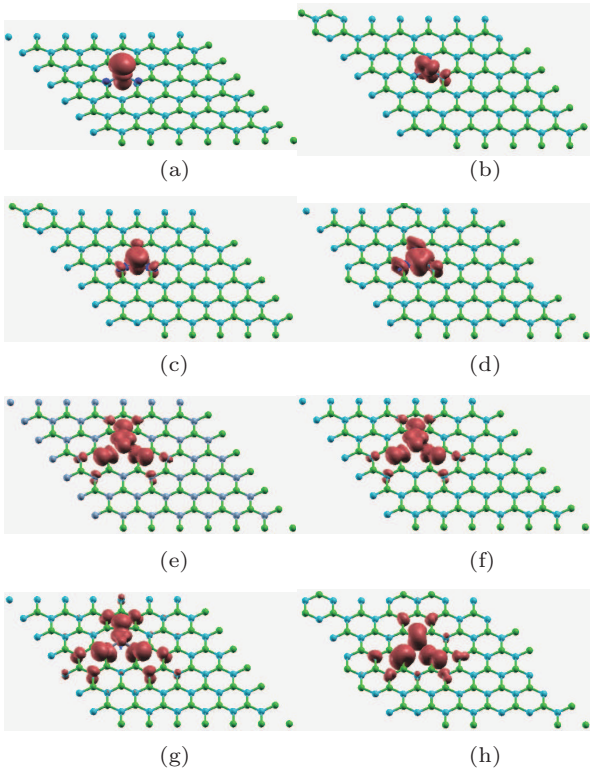


Fig. 7. (color online) Spin density maps of (a) Hf_{Al}, (b) W_{Al}, (c) Re_{Al}, (d) Os_{Al}, (e) Pt_{Al}, (f) Au_{Al}, (g) Hg_{Al} and (h) V_{Al} sheets (spin-up is shown in red and spin-down in blue).

4. Conclusion

The geometry, electronic structure and magnetic properties of 5d atoms doped h-AlN sheets are investigated using first-principles calculation methods. Different doped systems have different total magnetic moments. The total DOS, spin density maps, 5d orbital splits and molecular orbital analysis results are all illustrated, with obvious impurity levels shown in the DOS of the doped system. In our research, the geometries of all doped systems tend to have the C_{3v} or D_{3h} symmetry. In detail, Ta_{Al}, W_{Al}, Re_{Al}, Os_{Al} and V_{Al} tend to have a D_{3h} symmetry, Lu_{Al}, Hf_{Al}, Ir_{Al}, Pt_{Al}, Au_{Al} and Hg_{Al} tend to have a C_{3v} symmetry, while W_{Al}, Os_{Al}, Pt_{Al} and V_{Al} deviate from strict symmetries. The influence of symmetry and symmetry-breaking on the electronic structure and magnetic moment has been analyzed.

References

[1] Novoselov K S, Geim A K, Morozov S V, Jiang D, Zhang Y, Dubonos S V, Grigorieva I V and Firsov A A 2004 *Science* **306** 666
[2] Greber T 2010 *J. Surf. Sci. Nanotech.* **8** 62
[3] Iijima S 1991 *Nature* **354** 56
[4] Novoselov K S, Jiang D, Schedin F, Booth T J, Khotkevich V V, Morozov S V and Geim A K 2005 *Proc. Natl. Acad. Sci. USA* **102** 10451
[5] Rubio A, Corkill J L and Cohen M L 1994 *Phys. Rev. B* **49** 5081
[6] Prinz G A 1998 *Science* **282** 1660
[7] Araki Y, Yamaguchi M and Ishikawa F 2013 *Nanotechnology* **24** 065601
[8] Hao Y J, Cheng Y, Wang Y J and Chen X R 2007 *Chin. Phys.* **16** 217
[9] Lu L Y, Chen X R, Yu B R and Gou Q Q 2006 *Chin. Phys.* **15** 802
[10] Zhang Z F, Zhou T G and Zuo X 2013 *Acta Phys. Sin.* **62** 083102 (in Chinese)
[11] Hestroffer K, Mata R, Camacho D, Leclere C, Tourbot G, Niquet Y M, Cros A, Bougerol C, Renevier H and Daudin B 2010 *Nanotechnology* **21** 415702
[12] Hounjet L J, Caputo C B and Stephan D W 2013 *Dalton Transactions* **42** 2629
[13] Kirste R, Wagner M R, Nenstiel C, Brunner F, Weyers M and Hoffmann A 2012 *Phys. Status Solidi A* **210** 285
[14] Taniyasu Y, Kasu1 M and Makimoto T 2006 *Nature* **441** 325
[15] Li Y F, Zhou Z, Shen P, Zhang S B and Chen Z F 2009 *Nanotechnology* **20** 215701
[16] Landré O, Fellmann V, Jaffrennou P, Bougerol C, Renevier H, Cros A and Daudin B 2010 *Appl. Phys. Lett.* **96** 061912
[17] Oto T, Banal R G, Kataoka K, Funato M and Kawakami Y 2010 *Nature Photon.* **4** 767
[18] Cai Y X and Xu R 2010 *Chin. Phys. Lett.* **27** 096402
[19] Zhang L M, Fan G H and Ding S F 2007 *Acta Phys. Chim. Sin.* **23** 1498
[20] Qiao Z J, Chen G D, Ye H G, Wu Y L, Niu H B and Zhu Y Z 2012 *Chin. Phys. B* **21** 87101
[21] Zhang W, Cheng Y, Zhu J and Chen X R 2009 *Chin. Phys. B* **18** 1207
[22] de Almeida Junior E F, de Brito Mota F, de Castilho C M C, Kakanakova- Georgieva A and Gueorguiev G K 2012 *Eur. Phys. J. B* **85** 48
[23] Shitade A, Katsura H, Kuneš J, Qi X L, Zhang S C and Nagaosa N 2009 *Phys. Rev. Lett* **102** 256403
[24] Zhang H B, Lazo C, Blügel S, Heinze S and Mokrousov Y 2012 *Phys. Rev. Lett.* **108** 056802
[25] Hu J, Alicea J, Wu R Q and Franz M 2012 *Phys. Rev. Lett.* **109** 266801
[26] Kohn W and Sham L J 1965 *Phys. Rev.* **140** 1133
[27] Hohenberg P and Kohn W 1964 *Phys. Rev.* **136** 864
[28] Litinsky A O and Novikov S I 2012 *Russian Physics Journal* **55** 752
[29] Bessem B D, Chen J, Vivet A and PoiL ane C 2012 *J. Nanosci. Nanotechnol.* **12** 8635
[30] Yildirim A, Koc H and Deligoz E 2012 *Chin. Phys. B* **21** 037101
[31] Perdew J P, Burke K and Ernzerhof M 1996 *Phys. Rev. Lett.* **77** 3865
[32] Zheng F L, Zhang J M, Zhang Y and Vincent Ji 2010 *Physica B* **405** 3775
[33] Hou S M, Zhang J X, Shen Z Y, Zhao X Y and Xue Z Q 2005 *Physica E* **27** 45
[34] Gao X D, Jiang E Y, Liu H H, Mi W B, Li Z Q, Wu P and Bai H L 2007 *Appl. Surf. Sci.* **253** 5431
[35] Ran F Y, Subramanian M, Tanemura M, Hayashi Y and Hihara T 2009 *Appl. Phys. Lett.* **95** 112111